International Journal of Pharmaceutics 429 (2012) 148–157

Contents lists available at SciVerse ScienceDirect

International Journal of Pharmaceutics

journal homepage: www.elsevier.com/locate/ijpharm

Pharmaceutical Nanotechnology

Drug eluting sutures: A model for *in vivo* estimations

Tommaso Casalini, Maurizio Masi, Giuseppe Perale*

Dipartimento di Chimica, Materiali e Ingegneria Chimica "Giulio Natta", Politecnico di Milano, Via Mancinelli 7, 20131 Milano, Italy

ARTICLE INFO

Article history:
Received 19 January 2012
Received in revised form 12 March 2012
Accepted 13 March 2012
Available online 22 March 2012

Keywords:
Mathematical modeling
Drug delivery
Pharmaceuticals
Biopolymers
Suture threads

ABSTRACT

This work is focused on the development of a transient 1-dimension model to describe drug release from a bioresorbable suture thread in a living tissue and the pharmacologic behavior of the active substance being delivered from the device into the tissue. The model is based on fundamental conservation laws, represented by mass balances, being the thread degradation described through population balances and involving detailed hydrolysis kinetics. Monomer, water and drug diffusion are assumed as Fickian, and the increasing of diffusion coefficient is expressed with the "free volume" theory. Drug behavior in tissue is described with a "diffusion and reaction" approach. The model leads to a system of partial differential equations solved by applying the method of lines and then numerically integrated. Simulations allowed to estimate release dynamics and drug behavior in tissue and to obtain spatial and temporal profiles of drug in tissue. Moreover, phase diagrams, which show drug effect in time and space, are here introduced for the first time.

© 2012 Elsevier B.V. All rights reserved.

1. Introduction

The extremely wide success of bioresorbable devices was made possible thanks to polymers such as polylactic acid (PLA), polyglycolic acid (PGA) and poly-ε-caprolactone (PCL) which are commonly used in many medical devices because of their capability to degrade *in situ*, thanks to simply hydrolysis mechanism. An important application of this class of materials is surely represented by devices for controlled release of drugs, factors, proteins, DNA and genes (DuBose et al., 2005; Miller-Chou and Koenig, 2003; Sokolsky-Papkov et al., 2007; Tessmar and Gopferich, 2007; Willerth and Sakiyama-Elbert, 2007): indeed, while the device is subjected to degradation, it releases *e.g.* an active principle which diffuses out of the polymeric matrix to the local target tissue surrounding the device. The idea of drug delivery systems dates back to the '1960s, when devices of polyethylene or silicone rubber were used: these systems needed to be removed surgically due to their poor biodegradability, a strong limit to their utilization (Freiberg and Zhu, 2004). Nowadays, bioresorbable medical devices are an established reality, widely studied in literature (Fredenberg et al., 2011). Phenomena involved in degradation and drug release from such devices are several, as the overall system behavior is the result of their mutual influence (Alexis, 2005; Alexis et al., 2005; Arosio et al., 2008; Freiberg and Zhu, 2004; Grassi et al., 2008; Siegel et al., 2006; Westedt et al., 2006). The polymer nature determines its hydrophilicity and crystallinity, which influence water uptake and thus degradation dynamics. A hydrophilic and amorphous material degrades faster than a hydrophobic and crystalline one. Process dynamics is also influenced by molecular weight: a heavy polymer degrades slower because of a lesser water uptake. While water diffuses into the matrix, degradation occurs because of hydrolysis of ester bonds located along the chains. Resulting acid oligomers diffuse within and out the matrix, and act as catalysts for the hydrolysis reaction, which is favored by acid environment. Drug active terminals can also influence degradation (speeding or slowing the process) depending on their interaction with the reaction (Freiberg and Zhu, 2004; Siegel et al., 2006; Westedt et al., 2006). Two different degradation mechanisms can be distinguished (Alexis, 2005). If water diffusion is faster than de-polymerization kinetics, a uniform degrade of the entire matrix takes place and the process is called homogeneous or bulk degradation. *Vice versa*, when hydrolysis is faster than water diffusion, heterogeneous or superficial degradation occurs: hydrolysis involves only the surface, whilst the core remains intact. Heterogeneous behavior is strongly related to the dimension of the matrix: there is a critical thickness which discriminates between the two mechanisms (Grizzi et al., 1995; von Burkersroda et al., 2002). As regards drug delivery, it is generally accepted that drug release from a resorbable matrix depends both on device degradation and drug diffusion through the polymeric system. While degradation takes place, new diffusion paths are created because polymer chains become shorter and more distant each other; this phenomenon improves diffusion, and thus diffusion coefficient increases dynamically as hydrolysis occurs (Alexis, 2005; Alexis et al., 2005; Arosio et al., 2008; Freiberg and Zhu, 2004; Grassi et al., 2008; Pitt, 1992; Siegel et al., 2006; Westedt et al., 2006). Recently, a better reliability in drug delivery devices has

* Corresponding author. Tel.: +39 02 2399 3145; fax: +39 02 2399 3180.
E-mail address: giuseppe.perale@polimi.it (G. Perale).

0378-5173/$ – see front matter © 2012 Elsevier B.V. All rights reserved.
doi:10.1016/j.ijpharm.2012.03.024

Nomenclature

a	specific surface
$C_{b,i}$	bulk molar concentration of the ith specie
C_D	drug molar concentration in polymeric matrix
$C_{D,T}$	drug molar concentration in tissue
C_M	monomer molar concentration
C_n	n-long polymeric chain molar concentration
C_W	water molar concentration
D_i^0	diffusion coefficient of the ith specie in pure water
D_D	drug effective diffusion coefficient through polymeric matrix
D_M	monomer effective diffusion coefficient through polymeric matrix
$D_{D,T}$	drug diffusion coefficient through tissue
$D_{D,W}$	drug diffusion coefficient in water
D_W	water effective diffusion coefficient through polymeric matrix
K_{EQ}	polymerization reaction thermodynamic equilibrium constant
k_C	mass transport coefficient
$k_{C,T}$	mass transport coefficient
k_D	depolymerization kinetic constant
k_P	polymerization kinetic constant
k_{hydr}	lidocaine hydrolysis kinetic constant
k_T	tissue kinetic constant
MW_{drug}	drug molecular weight
MW_{MON}	monomer molecular weight
MW_n	numeral average molecular weight
MW_w	weight average molecular weight
P_n	n-long polymeric chain
PD	polydispersity
r	thread radius
r_{eq}	equivalent radius
r_P	reaction rate
r_t	tissue radius
Sh	Sherwood number
$t_{1/2}$	drug half life time
V_t	thread volume
W	water

Greek symbols

β	bioavailability
μ_0	zeroth order moment
μ_1	first order moment
μ_2	second order moment
ρ_{pol}	polymer density
$\tau_{,i}$	characteristic diffusion time of the ith specie

become an inescapable necessity, and this encouraged researchers to replace the "trial and error" *modus operandi* with a new model based approach (Grassi et al., 2008). Indeed, on the modeling side, literature offers a wide variety of models, both on polymer degradation and release processes, also coupling these phenomena in order to obtain a complete description of the system. However, degradation dynamics is often described in a simple way with a first order reaction, and diffusion phenomena are considered as Fickian; diffusion coefficient is kept constant or expressed with the free volume theory. It is also observed that these models are often related to drug filled capsule o films instead of drug-polymer compounded matrices (Colombo et al., 1996; Crow et al., 2005; Faisant et al., 2002; Grayson et al., 2005; Musial et al., 2010; Noorsal et al., 2005; Pitt, 1992; Siegel et al., 2006; Siepmann and Gopferich, 2001; Thombre and Himmelstein, 1985; Tojo et al., 1998; Westedt et al., 2006) even if there are examples of more complex geometries too (Helbling et al., 2011). The attention is also focused on the distinction between bulk and surface degradation, developing models which are able to describe and distinguish both mechanisms (Rothstein et al., 2009; Soares and Zunino, 2010). It must be noticed, however, that most relevant advancements in polymer matrices and drug release modeling have been recently reviewed (Kaunisto et al., 2011; Lao et al., 2011; Sackett and Narasimhan, 2011).

For what concerns suture threads, which are the subject of this work, some attempts to model these devices are already present in literature (Arosio et al., 2008; Perale et al., 2009, 2010; Zurita et al., 2006a,b). Zurita et al. (2006a,b) studied release of triclosan and ibuprofen from mono and multi-filament sutures, by means of regression-based mathematical models. Arosio et al. (2008) proposed a model based on mass balances and population balances coupled with a shrinking core approach, which described both device degradation and drug release; this model was enhanced by Perale et al. (2009, 2010) who explicitly introduced diffusive phenomena through Fick's law.

As regards to drug dynamics *in vivo*, on the other hand, literature offers only few examples of mathematical models. Krewson and Saltzman (1996) and Saltzman et al. (1999) used a diffusion and reaction approach to model the delivery of recombinant human nerve growth factor (rhNGF) in adult rat brain; in particular, they proved the consistency of a model involving a Fickian diffusion and a first order drug elimination kinetics when applied to the investigation of drug behavior in living tissues. Kretsos et al. (2004) described percutaneous adsorption of a drug with a one dimensional model, which takes into account diffusion through the skin and vascular clearance. Skin was divided in several layers, with their own values of diffusion coefficient and partition constant. Loney and Susarla (2009) modeled lidocaine release from poly lactic-co-glycolic acid (PLGA) spherical particles, taking into account the effect of drug absorption rate on the release kinetics. Kim and Simon (2011) modeled drug delivery patches loaded with a corticosterone, taking into account transport phenomena through both the patch and the skin; they also proposed an approach to optimize device design. Kuttler et al. (2010) used a computational fluid dynamics (CFD) approach in order to simulate drug distribution into cerebrospinal fluid along spinal cord. Grassi et al. (2010) developed a model able to describe *in vivo* drug release, absorption, distribution, metabolism and elimination after oral administration. Shin et al. (2011) predicted the tissue distribution and pharmacokinetics of apicidin in rats, mice and human through a physiologically based pharmacokinetic modeling.

There are also other efforts for what concerns the modeling in *in vivo* environment; Monkare et al. (2010) studied the *in vivo* degradation of poly(ester anhydride)-based devices, highlighting a surface erosion controlled drug release in rat model. Semete et al. (2010) evaluated the biodistribution of PLGA nanoparticles in Balb/C mice model, while Lee et al. (2010) focused their attention on poly(ethylene glycol)-block-poly(ε-caprolactone) nanoparticles in the same animal model.

Drug delivery *in vivo* experimental data are scarcely available, mainly for the extreme complexity of providing quantitative monitoring of both delivery and clearance phenomena (Butts et al., 2009; Batheja et al., 2011; Dee et al., 2002; Perale et al., in press). Mostly fluorescent substances, including some drugs, are used as delivered molecules, but the need of having light-transparent animal models requests the choice of very small animals, *e.g.* zebra fish (Li et al., 2011), thus strongly limiting the possibility to extend obtained results into clinics. Nevertheless, it is worth to notice that Garcia et al. (2011), using PLGA nanoparticles, showed that encapsulated bupivacaine was able to give a longer in vivo analgesic effect in rats. Moreover, Perale et al. (in press) studied the in vivo delivery

kinetics of different drugs along the spinal cord of injured mice using the non invasive Explore Optix System technique. Hence, in this framework, both the scientific and industrial trends point toward the development of physical-chemical sound meaning models, also to predict drug release behavior in *in vivo* context. Saving time and expensive long lasting animal trials keep the pace with ethical concerns and recent indications towards the reduction of animal use in scientific studies, particularly where computational instruments offer viable, cheap and trustful tools for complex simulations (Siepmann et al., 2006). Aim of the present work was, thus, to specifically develop a model describing the behavior of a bioresorbable suture thread loaded with lidocaine hydrochloride, an anesthetic commonly used in surgery (Remington, 1995), that serves as a tool to easily design smart sutures performing desired release profiles. Degradation process is here described using fundamental conservation principles: *i.e.* it means that model has a mechanistic nature, thus involved parameters have a physical sound meaning (kinetic constant, diffusion coefficient, *etc.*) and can be estimated independently. In particular, population balances are used in order to obtain a detailed description of polymeric chains decomposition. Mass balances take into account diffusive phenomena, since oligomers can diffuse within and out the matrix. Conservation equations are also written for monomer, water, and drug. Diffusion coefficient is expressed according to the free volume theory (Vrentas and Vrentas, 1998), thus model takes into account the enhanced diffusion due to degradation process. Moreover, the system can be substantially considered as isothermal, and thus energy balance is not needed. For sake of simplicity, the model solution is here presented under cylindrical symmetry, but this restriction can be easily removed by simply changing Laplacian form.

Starting point of this work was the previously cited model developed by Perale et al., which was chosen also for its validated results (Lao et al., 2011; Perale et al., 2010; Sackett and Narasimhan, 2011). First of all, the here presented describes drug release from a bioresorbable suture thread directly into a living tissue and the behavior of the drug in the tissue. The drug behavior is described with a "diffusion and reaction" approach, where the active principle diffuses through the tissue (following Fick law) (Saltzman et al., 1999) and during its diffusion it is also metabolized by the organism. Moreover, diffusion phenomena into device are described in a more detailed way, since the diffusion enhancement due to the thread degradation is explicitly taken into account.

2. Model development

The polymeric suture thread was here considered as a semi-batch reactor with constant volume, as far as degradation process follows a homogeneous behavior. Tissue is supposed cylindrical, for the sake of simplicity, where suture thread coincides with the axis of this cylinder. Suture thread is also supposed to be surrounded by a thin layer of water, which constitutes the interface between thread and tissue; this is representative of the influx of liquid due to the initial inflammatory response, because of the foreign body implantation (Dillow and Lowman, 2002). In regard to the suture thread, model describes diffusion of water, monomer and drug through the matrix. Water penetrates into the matrix (which swells) and breaks the long chains into oligomers, which can then diffuse through and out of the matrix (Li et al., 1990). However, since oligomers diffusion coefficient value is very low, only monomer diffusion is taken into account (Perale et al., 2009). Polymer degradation is described with a reversible polycondensation reaction, which takes place in large excess of water:

$$P_n + P_m \leftrightarrow P_{n+m} + W \tag{1}$$

This kinetic scheme can be expressed in detail through mass balances, thanks to population balances (Ramkrishna, 2000). Degradation is an auto-catalytic process, where the role of the catalyst is played by weakly acid oligomers which hardly diffuse into the matrix and thus create an acid environment due to their carboxylic terminals (Li et al., 1990). Moreover, water also causes solubilization of drug particles dispersed into the device. Solubilized drug can diffuse towards the tissue through the matrix. The active principle then diffuses into the tissue, where is metabolized. This physiologically contributes to maintain an adequate driving force for diffusion between the inner core of the filament and the outer tissue.

2.1. Polymer degradation

Polymer degradation must be taken into account, because effective diffusion coefficient increase is directly linked to the decrease of molecular weight. According to kinetic scheme (1), a water molecule can break a long polymeric chain in two smaller fragments; however, only monomer and water can diffuse through the matrix. These phenomena allow writing the following conservation equations for monomer and water, respectively:

$$\frac{\partial C_M}{\partial t} = \frac{1}{r}\frac{\partial}{\partial r}\left(D_M r \frac{\partial C_M}{\partial r}\right) - 2k_P C_M \sum_{n=1}^{\infty} C_n + 2\frac{k_P}{K_{EQ}} C_W \sum_{n=2}^{\infty} C_n \tag{2}$$

$$\frac{\partial C_W}{\partial t} = \frac{1}{r}\frac{\partial}{\partial r}\left(D_W r \frac{\partial C_W}{\partial r}\right) + k_P \sum_{n=1}^{\infty} C_n \sum_{m=1}^{\infty} C_m - \frac{k_P}{K_{EQ}} C_W \sum_{n=1}^{\infty} (n-1) C_n \tag{3}$$

where C_M, C_W, C_n are the molar concentration of monomer, water, and a generic n-long chain respectively, D_M and D_W are the effective diffusion coefficient of monomer and water in the polymeric matrix, r is the thread radius, k_p is the polymerization constant and K_{EQ} is the equilibrium constant of the reaction. As regards monomer equation, the first term represents the monomer units, which diffuse out from the solid matrix: a Fickian diffusion is assumed. The conservation equation for a generic polymer chain with n monomeric units (with $n > 1$) can also be written as follows:

$$\frac{\partial C_n}{\partial t} = k_P \sum_{j=1}^{n-1} C_j C_{n-j} - 2k_P C_n \sum_{j=1}^{\infty} C_j + 2\frac{k_P}{K_{EQ}} C_W \sum_{j=n+1}^{\infty} C_j - \frac{k_P}{K_{EQ}} C_W (n-1) C_n \tag{4}$$

In order to simplify the model (which would lead to a large system of differential equations), method of moments is applied and mass balances are written in terms of statistical moments of order zero, one and two, where the generic kth order moment is defined as follows (Ramkrishna, 2000):

$$\mu_K = \int_0^{\infty} n^K f_N(n) dn = \sum_{n=1}^{\infty} n^K C_n \tag{5}$$

After some computations, especially with regard to summations (Goldstein and Amundson, 1965), a simpler system can be obtained, where the conservation equation for a generic *n-long* chain is substituted with three equations which describe evolution in time of first three order moments. Monomer and water equations are also written in terms of statistical moments, and the resulting system is the following:

$$\frac{\partial C_M}{\partial t} = \frac{1}{r}\frac{\partial}{\partial r}\left(D_M r \frac{\partial C_M}{\partial r}\right) - 2k_P C_M \mu_0 + \frac{k_P}{K_{EQ}} C_W (\mu_0 - C_M) \tag{6.a}$$

$$\frac{\partial C_W}{\partial t} = \frac{1}{r}\frac{\partial}{\partial r}\left(D_W r \frac{\partial C_W}{\partial r}\right) + k_P \mu_0^2 - \frac{k_P}{K_{EQ}} C_W(\mu_1 - \mu_0) \quad (6.b)$$

$$\frac{\partial \mu_0}{\partial t} = \frac{1}{r}\frac{\partial}{\partial r}\left(D_M r \frac{\partial C_M}{\partial r}\right) - k_P \mu_0^2 + \frac{k_P}{K_{EQ}} C_W(\mu_1 - \mu_0) \quad (6.c)$$

$$\frac{\partial \mu_1}{\partial t} = \frac{1}{r}\frac{\partial}{\partial r}\left(D_M r \frac{\partial C_M}{\partial r}\right) \quad (6.d)$$

$$\frac{\partial \mu_2}{\partial t} = \frac{1}{r}\frac{\partial}{\partial r}\left(D_M r \frac{\partial C_M}{\partial r}\right) + 2k_P \mu_1^2 + \frac{k_P C_W}{3K_{EQ}}\left(\mu_1 - 2\frac{\mu_2^2}{\mu_1} + \frac{\mu_2 \mu_1}{\mu_0}\right) \quad (6.e)$$

It must be noted that the effective diffusion coefficients must be included into derivative operator, since, as mentioned at the beginning, they depend on molecular weight, which varies along the radius because of degradation phenomena. Diffusion coefficients, indeed, are directly related to average molecular weight thanks to free volume theory, as explained in the parameters estimation section (*vide infra*).

The moments of the first three orders have a specific physical meaning: the zeroth order moment represents the number of chains for an unit volume; the first order moment represents the overall chain length for an unit volume, and the second order moment is related with the polydispersity of chain length distribution function (Ramkrishna, 2000). Thanks to statistical moments, it is possible to compute properties of interest such as average molecular weight, which, as mentioned, intervenes in the computation of effective diffusion coefficients.

As regards boundary conditions for monomer and water, profile symmetry is imposed at the thread centre, while at the interface thread/water the continuity of matter flux at the interface is imposed. In this case, the entire tissue is considered as water. Mass transfer coefficient k_c can be computed with Higbie theory (Bird et al., 2002); for this system, Sherwood number is equal to $8/\pi$.

Initial conditions for monomer and water concentrations are equal to zero, because device is supposed to be anhydrous and without monomer residuals. Initial conditions for statistical moment are referred to unperturbed polymer. Detailed formulas are presented in supporting information.

2.2. Drug release

The model assumes that drug diffusion follows a Fickian behavior; drug particles are reasonably assumed to be uniformly dispersed in the thread section (Perale et al., 2010). Release mechanism can be explained as follows: water penetrates into the matrix and wets solid drug particles, which starts to solubilize accordingly with thermodynamic and kinetics of the process; solubilized drug can diffuse through polymeric matrix. For sake of simplicity, experimental data regarding a lidocaine releasing suture thread are here used as reference set (Perale et al., 2009, 2010): the maximum lidocaine concentration value that can be reached inside the thread, equal to the initial concentration value, is equal to 1.2 mg/cm^3, well below the solubilization limit (1.43 g/cm^3) (Remington, 1995). For this reason, drug solubilization dynamics is neglected, since it is assumed that there is an adequate driving force that implies the instantaneous dissolution. Reliability of this hypothesis has already been achieved (Perale et al., 2009, 2010). Drug conservation equation is the following:

$$\frac{\partial C_D}{\partial t} = \frac{1}{r}\frac{\partial}{\partial r}\left(D_D r \frac{\partial C_D}{\partial r}\right) \quad (7)$$

where C_D is drug concentration in the thread and D_D is drug effective diffusion coefficient in the polymeric matrix. Effective diffusion coefficient, as said, must be included in derivative operator since it depends on molecular weight, which varies along thread radius. One boundary condition involves profile symmetry at the thread centre; the other boundary condition is calculated by imposing the continuity of material flux at the thread interface, considering drug concentration in the thin layer of water, which surrounds the thread. However, it must be noted that this value is not a constant number, since it depends both on thread release and tissue diffusion dynamics. Thus, another equation is needed to take into account these phenomena:

$$\frac{\partial C_{b,D}}{\partial t} = k_{C,D} \cdot a \cdot (C_D - C_{b,D}) - k_{C,T} \cdot a \cdot (C_{b,D} - C_{D,T}) \quad (8)$$

where C_D and $C_{D,T}$ are the values of drug concentration at thread/water and water/tissue interfaces, respectively, a is the specific mass transfer surface and $k_{C,T}$ is the mass transfer coefficient related to water/tissue flux, computed by means of penetration theory as explained before. Specific surface term is equal for both mass fluxes, since the volume of water thin layer is considered to be negligible. Drug concentration in water increases because of the release from the thread, and decreases because of gradient-driven diffusion into the tissue. Moreover, drug concentration in this layer is always lower than solubilization limit.

2.3. Drug behaviour in tissue

Drug behaviour in tissue is described by a "diffusion and reaction" approach (Anissimov and Roberts, 2011; Siepmann et al., 2006); solubilized drug diffuses into the tissue where it is metabolized, and thus eliminated, according to a first order reaction; moreover, tissue vascularization is neglected:

$$\frac{\partial C_{D,T}}{\partial t} = D_{D,T}\frac{1}{r}\frac{\partial}{\partial r}\left(r\frac{\partial C_{D,T}}{\partial r_T}\right) - k_T C_{D,T} \quad (9)$$

where $D_{D,T}$ is the diffusion coefficient of the drug in the tissue, r_t is the radius of the tissue (supposed cylindrical, for the sake of simplicity), k_T is the first order kinetic constant of drug metabolization and $C_{D,T}$ is drug concentration in tissue. Drug consumption dynamics have been assumed to follow a first order kinetic law, because of the low involved amount of drug (Birkett, 2002). The consistency of such kinetic law has already been showed in literature (Krewson and Saltzman, 1996). Boundary condition at the tissue/thread interface is the mass conservation between the thin layer of water that surrounds the thread and the tissue. Initial value of drug in tissue is equal to zero.

2.4. Thread geometrical approximation

In real applications, suture thread length is greater than wound length; usually, the ratio between thread length and wound length is usually equal to 2–2.5: in a wound closure, the suture thread is not perfectly straight, but it is indeed tied several times into various stitches or knots. This geometry can be modeled as a series of cylinders and spheres, which respectively represent the thread segments and the knots. In order to avoid a complex geometrical modeling, which also would require other and unavailable input parameters (*e.g.* spheres radius *etc.*) and would thus require the introduction of severely imprecise approximations, another geometrical modeling approach must be considered, anyhow avoiding any loss of generality. An equivalent radius (*i.e.*, a radius obtained considering a suture thread with the same mass of the original one, and a length equal to the wound length) is not suitable because the radius effect on drug release is very strong. Geometry role was thus modeled by multiplying the diffusive flux, which comes from the

thread (and then the flux which is seen by the tissue), by the ratio between the thread length and the wound length. All simulations were thus carried out under this assumption.

2.5. Model parameters estimation

Parameters involved, *i.e.* polymer degradation kinetics (*i.e.*, k_p, K_{EQ}) and drug metabolization kinetics (k_T), are essentially related to diffusion phenomena (both in thread and in tissue). Degradation kinetics parameters depend on chosen polymer; in particular, this work is focused on suture threads made of poly-ε-caprolactone but without any loss of generality: indeed, the here developed model can be easily applied to any other biodegradable polymers. Parameters adopted are summarized in Table 1 (Frank et al., 2005; Haik-Creguer et al., 1998; Siegel et al., 2006; Zurita et al., 2006a,b). As regards diffusion coefficients, it is difficult to estimate reliable values in a solid matrix because a reliable theory is not yet available (Bird et al., 2002; Crank and Park, 1968), whilst a prediction in gases and liquids is more consolidated (Bird et al., 2002). Nowadays, the theory which seems to offer the best results and the highest reliability is the "free volume theory" (Vrentas and Vrentas, 1998). Model assumes an expression of diffusion coefficient which is related to numeral average molecular weight (Streubel et al., 2000):

$$D = \frac{12}{25} D_i^0 \exp\left(2.5\left(1 - \frac{MW_n(t,r)}{MW_n(t=0)}\right)^{0.5}\right)$$

$$i = monomer, water, drug \tag{10}$$

where D_i^0 is the diffusion coefficient in pure water and MW_n is the number average molecular weight; thus, since numeral average molecular weight depends on time and space, also the effective diffusion coefficient varies, as said, with time and space.

Drug kinetic constant in tissue can be calculated starting from a drug administration by injection (Birkett, 2002); assuming a linear kinetics (hypothesis acceptable due to low concentrations) a simple mass balance can be written and analytically solved:

$$\frac{dC}{dt} = -k_T \beta C \tag{11.a}$$

$$C = C_0 \exp(-k_T \beta t) \tag{11.b}$$

where C_0 is initial concentration of drug and β is drug bioavailability. Drug bioavailability is "the rate and extent to which the active drug is absorbed from a pharmaceutical form and becomes available at the site of drug action" (Grassi et al., 2008). In other words, bioavailability is the fraction of the drug that reaches the systemic circulation; indeed, the partial absorption and the effects of the metabolism reduce the amount of active principle, which is really available: bioavailability numerical value is hence comprised between 0 and 1, *i.e.* between 0 and 100%. The aforementioned factors intervene when oral, rectal or transdermal administration are made, but they do not in case of intravenous injection, because the entire amount of drug reaches the systemic circulation; thus, in this case, β is equal to 1. It must be noted that this situation can approximate the release from suture thread, because drug reaches the tissue directly and it is not subjected to clearance. Since drug half life time $t_{1/2}$ is a known value (Goodman et al., 2006), equal to 2 h, kinetic constant can be simply calculated:

$$k_T = \frac{\ln 2}{t_{1/2}} \tag{12}$$

Water diffusion coefficient in a biological tissue is in the order of 10^{-5} cm^2/s (Pavlisa et al., 2009) when water self diffusion coefficient at 36.6 °C is 2.49×10^{-5} cm^2/s (Posnansky and Shah, 2008). As regard to lidocaine, literature reports a diffusion coefficient value related to the *stratum corneum*, equal to 5×10^{-8} cm^2/s (Mitragotri, 2000). However, the here presented system is constituted by a solubilized drug that mainly diffuses in a muscular tissue, which has a much greater permeability than the *stratum corneum*, whose function is indeed to protect the derma from external agents. Meriani et al. (2004) studied diffusion of nimesulide (MW = 308.311 g/mol) through rat intestine and a diffusion coefficient of 10^{-6} cm^2/s was found from model fitting. Saltzman et al. (1999) studied intracranial delivery of recombinant human nerve growth factor (a protein whose molecular weight is in the order of 20 kDa (Song et al., 2007)) and found a diffusion coefficient of 8×10^{-7} cm^2/s in the brain, *versus* a diffusion coefficient in water equal to 1.3×10^{-6} cm^2/s reported by the same author. Wang et al. (2005) studied diffusion of fluorescein (a drug mimetic compound, with a molecular weight of 376 g/mol) in bone and found a diffusion coefficient of 3.3×10^{-6} cm^2/s. Since lidocaine is more similar to nimesulide and to fluorescein for what concerns molecular weight (MW = 234.34 g/mol for lidocaine) and steric hindrance, an estimation of lidocaine diffusion coefficient in tissue of 10^{-6} cm^2/s can reasonably be consistent with available data and thus realistic (see Table 1).

Table 1
Model input data.

Monomer molecular weight	MW_{MON} = 114.14 mg/mmol
Density	ρ = 1200 mg/cm^3
Polymer molecular weight	MW_n = 80,000 g/mol
Monomer effective diffusivity	$D_M = 10^{-10}$ cm^2/s
Water effective diffusivity	$D_W = 10^{-7}$ cm^2/s
Drug effective diffusivity (thread)	$D_D = 10^{-8}$ cm^2/s
Polymerization kinetic constant	$k_p = 3.6 \times 10^{-12}$ mmol/cm^3/h
Equilibrium constant	$K_{EQ} = 10^{-3}$
Polydispersity	PD = 1.2
Drug metabolization kinetic constant	k_T = 0.3466 1/h
Drug diffusivity (tissue)	$D_{D,T} = 10^{-6}$ cm^2/s

2.6. Environmental effects

Inflammation reaction, due to the presence of the device, induces macrophages activation and this implies a decreasing of environment pH value. A representative value of pH for such situation can be equal to 5; for example, Holy et al. (1999) studied degradation *in vitro* simulating *in vivo* conditions by maintaining the environment pH equal to 5. For what concerns device degradation, the main pH contribution is due to acidic oligomers inside the matrix (Alexis, 2005) and this is taken into account by the model; pH of surrounding medium is important only for very low values (Alexis, 2005). Enzymes role in polymer degradation in *in vivo* environment has been found to depend on polymer hydrophilicity and molecular weight (Alexis, 2005; Numata et al., 2008; Tsuji and Tezuka, 2004; Tsuji et al., 2005). In particular, enzymatic degradation becomes less important increasing polymer molecular weight and decreasing water uptake. Since the reference suture thread is made of PCL (that is not very hydrophilic) with a molecular weight of 80 kDa, and since the drug release time scale is much lower than the device degradation one, enzymatic contribution can be safely neglected. In literature, stability of lidocaine in aqueous solutions with respect to temperature and pH has been properly discussed (Kamaya et al., 1983; Powell, 1987; Sjoberg et al., 1996). Powell (1987) proposed hydrolysis mechanism of lidocaine, deriving an expression for kinetic constant which takes into account also pH dependence. In the system described by the model, the pH range can vary from a value of 4 (acidic environment inside the thread, due to acid oligomers) to a value of 7.4 (pH of extracellular fluids of the tissue in which drug diffuses). Moreover, as mentioned, a pH value of 5 can be representative of the inflammation reaction and macrophages activation (Holy et al., 1999). In this range of pH values and at a temperature of 310 K, hydrolysis kinetic constant varies

from $1.856 \times 10^{-12}\,s^{-1}$ to $1.005 \times 10^{-11}\,s^{-1}$; moreover, lidocaine p$K_a$ value is set equal to 7.57, *i.e.* its value at 310 K (Kamaya et al., 1983; Powell, 1987). These results allow to obtain characteristic times of lidocaine hydrolysis, that can be compared with characteristics time of diffusion (both in the tissue and in the thread) and consumption.

$$\tau_{hydr} = \frac{1}{k_{hydr}} = 5.39 \times 10^{11} - 9.95 \times 10^{11}\,s \quad (13)$$

$$\tau_{diff,thread} = \frac{r_{thread}^2}{D_D} = 22,500\,s \quad (14)$$

$$\tau_{diff,tissue} = \frac{r_{tissue}^2}{D_{D,T}} = 10^6\ s \quad (15)$$

$$\tau_{cons,tissue} = \frac{1}{k_T} = 10,387\,s \quad (16)$$

Hydrolysis characteristic times in the aforementioned pH range are at least five magnitude orders greater with respect to characteristic times of main involved phenomena; thus, lidocaine hydrolysis can be neglected. For the sake of completeness, it must be said that in extracellular fluids, and this at pH value equal to 7.4, equilibrium between protonated and unprotonated lidocaine form occurs; however, only unprotonated form is able to cross cellular membrane and thus to be effective (Goodman et al., 2006). Metabolization constant has been computed starting from half-life time of lidocaine, and thus it contains all kinetics information about the consequences of this equilibrium in lidocaine effectiveness.

2.7. Full model and numerical solution

All equations form a single complete system, because all phenomena are related each other: diffusion coefficient depends on the polymer degradation, which then influences the drug released from the thread and finally the drug that arrives into the tissue. Moreover, the driving gradient for the drug release from the thread depends also on the amount of drug present in the tissue. Thus, a system of PDEs was obtained, which was solved applying method of lines (LeVeque, 2007): spatial second order derivatives are approximated with the centred formulation, obtaining a large system of ODEs with respect to time. Resulting system is numerically integrated with ode15 s algorithm as implemented in MATLAB. Model consistency was verified through mass balances; details are reported in supporting information material.

3. Results and discussion

Simulations were carried out considering a real situation: in particular, a surgical removal of a naevus was examined. The skin was anesthetized with an excess of 1 cc of carbocaine solution 1% and wound was treated with three internal resorbable suture stitches and four external non resorbable ones. The average length of each stitch was 35 mm and thread diameter of internal stitches is 0.3 mm (*i.e.* United States Pharmacopeia "USP" 3-0). As said before, tissue is assumed as cylindrical, and its dimensions are computed considering the estimated anaesthetized tissue: a diameter of 20 mm and a length of 40 mm (data kindly provided by Gianpietro Sala, MD, private practitioner, Milan, Italy). Simulations have a triple purpose: (i) estimating the amount of released drug, (ii) evaluating the behavior of the active principle which diffuses in the tissue; and (iii) examining the effect of thread diameter on the two aforementioned aspects. First of all, it can be immediately seen that drug release dynamics in tissue and in water are remarkably different, as a result of the different driving gradient experienced by drug molecules in these two situations: in the first case, indeed, the drug diffuses in a tissue being eliminated with a certain kinetic and hence

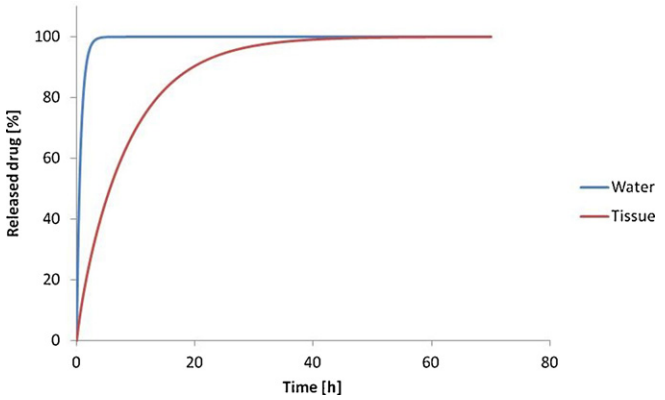

Fig. 1. Drug release in water and tissue environment.

does not experience a bulk concentration which, in the second case, is always kept null (Perale et al., 2009, 2010) (see Fig. 1).

3.1. Behavior in tissue

Another aim of simulations was to describe the behavior of the drug, which diffuses into the tissue, where it is then metabolized after having provided its effect and thus finally eliminated. Lidocaine can be toxic, anesthetic or analgesic depending on its concentration. This drug has analgesic effect when its concentration is comprised between 1.5 μg/ml (6.4×10^{-6} mmol/cm^3) and 3 μg/ml (1.28×10^{-5} mmol/cm^3). When concentration is under 1.5 μg/ml, lidocaine has not effect; if this is above 3 μg/ml an anesthetic effect is obtained. Maximum concentration allowed is 10 μg/ml (4.27×10^{-5} mmol/cm^3); for higher values, lidocaine has toxic effects. As said before, for the sake of the geometrical simplicity of the model, tissue is considered as cylindrical, with a radius of 10 mm and a length of 40 mm, according to the experimental measurements available. Suture thread coincides with cylinder axis. All further simulations were carried out considering a USP 3-0 suture thread with a molecular weight of 80,000 Da, according to available data, and with 1%, w/w of lidocaine loaded. Simulation inputs are summarized in Table 2.

Drug diffusion into the tissue can be seen as a wave that fades as time passes, because of drug consumption kinetics. Indeed, lidocaine concentration shows an initial peak due to bare diffusion, which decreases while drug is metabolized (Fig. 2).

Drug diffuses into the tissue, but it is also metabolized within the tissue and thus eliminated. Drug cannot manage to reach an effective concentration everywhere in the tissue, but only at a small distance from the thread. This can be easily seen observing temporal profiles (Fig. 3).

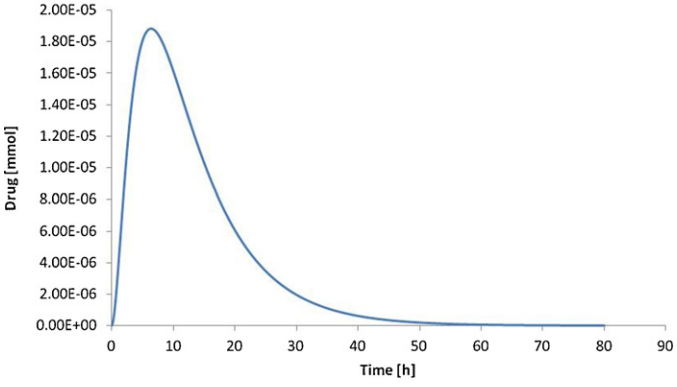

Fig. 2. Drug amount in tissue with respect to time.

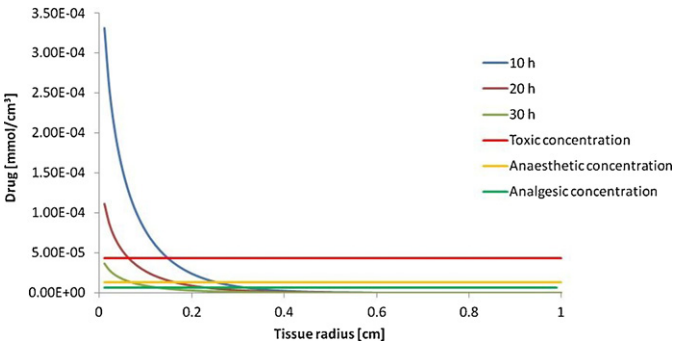

Fig. 3. Temporal profile of lidocaine release in tissue.

During the first seconds, lidocaine starts to diffuse into the tissue; diffusion rate is greater than consumption rate, because thread concentration is high. Drug is then able to reach tissue portions, which are relatively far from the thread, but it is not able to cover the entire wound volume. It must also be seen that near the device drug concentration is higher than the toxic one, and that the area potentially interested by toxic effect is a small fraction of the wound. As time passes, lidocaine diffuses in the tissue and it is consumed; moreover, its concentration in the thread obviously decreases because of release. After 30 h, temporal profiles, however, are not the most suitable way to evaluate device performances, because of their poor immediacy; for this reason, phase diagrams are introduced, as explained below.

Another result of interest is referred to the drug amount that must be loaded into the thread: lidocaine fraction cannot exceed 1–3%, w/w in order to avoid toxic effects. This requirement has positive drawbacks on device production, because a great drug amount in pellets makes their extrusion more difficult and can reduce thread mechanical properties such as *e.g.* tensile strength (Perale et al., 2008).

3.2. Phase diagrams and their application: smart thread design and application to a real case

Phase diagrams constitute the unification of the data provided by spatial profiles and temporal profiles. They show drug effect in time and space. In other words, they indicate *when* and *where* a certain effect is achieved: an example of phase diagram can be seen in Fig. 4 where data refer to a suture thread made of poly-ε-caprolactone, with a diameter of 0.3 mm and a molecular weight of 80,000 g/mol.

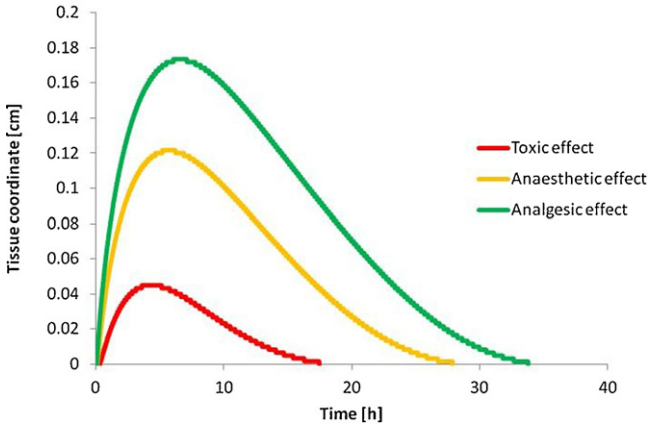

Fig. 4. Phase diagram (USP 3-0, *MW* = 80,000 g/mol, drug load = 1%, w/w).

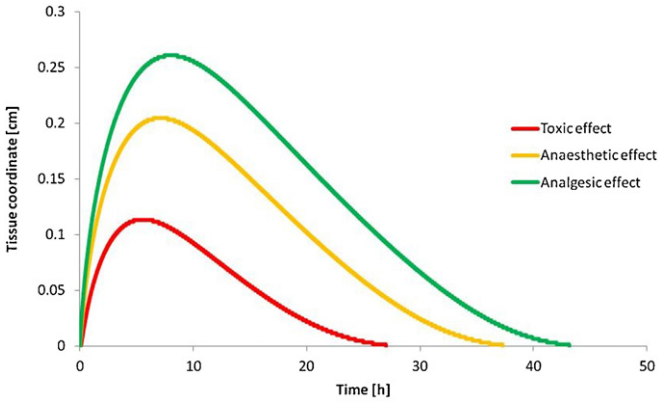

Fig. 5. Phase diagram (USP 3-0, *MW* = 80,000 g/mol, drug load = 3%, w/w).

The red line limits the area where drug has toxic effect, the yellow line bounds the area subjected to anaesthetic effect, while the green line represents minimum effective concentration of drug, and thus shows the limit beyond which drug has not effect. Moreover, drug effect can be easily quantified: the suture thread represented by this phase diagram provide an anaesthetic effect for about 28 h and an analgesic effect for about 34 h. As regard to tissue volume, the analgesic effect covers a maximum distance from the thread of about 0.18 cm, while the anaesthetic effect interests a maximum distance from the thread of about 0.12 cm. Hence, when the thread already exists as in this specific case, the phase diagram can offer an immediately evident snapshot of device efficiency, useful also for medical staff. On the other hand, when a suture thread has to be designed with the aid of simulations, phase diagrams can be the starting point to perform a fast and cheap device optimization. Indeed, it can be readily seen that the device under investigation is able to give relief from post surgical pain for more than one day, but the effect interests only a limited wound volume. Increasing drug load to 3% (Fig. 5), that is the upper allowed limit in order to perform pellet extrusion, device effect is prolonged both in terms of time and space.

Such device provides an analgesic effect for about 42 h, covering a maximum distance of about 0.27 cm, while the anaesthetic effect lasts until about 38 h and reaches a distance of about 0.2 cm. Again, thanks to phase diagrams, thread performances can be easily evaluated: while the relief against post surgical pain is prolonged in time and space, also toxic effects become more relevant.

However, as mentioned, the starting point for the simulation was a real example involving surgical removal of a naevus, whose data are reported in Table 2. In particular, the tissue was anesthetized with carbocaine before the application of the suture thread, while in the previous computations the initial drug concentration in the tissue was put equal to zero. In order to reproduce in a more adherent manner the real situation, a simulation was carried out considering an initial drug concentration in the tissue equal to twice the minimum anesthetic lidocaine concentration, which interests a distance from the thread of 2 cm. Indeed, since carbocaine properties are similar to lidocaine ones (Goodman et al.,

Table 2
Simulation input data.

Thread diameter	0.03 cm
Thread length	10.5 cm
Thread volume	7.42×10^{-3} cm^3
Lidocaine molecular weight	234.34 mg/mmol
% loaded lidocaine	1%, w/w
Initial lidocaine concentration	5.1×10^{-2} mmol/cm^3
Wound length	4 cm
Wound diameter	2 cm

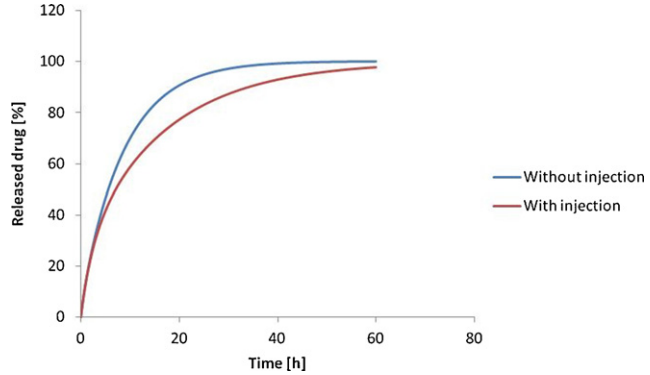

Fig. 6. Release profiles for a USP 3-0 suture thread with respect to initial presence of drug in the target tissue.

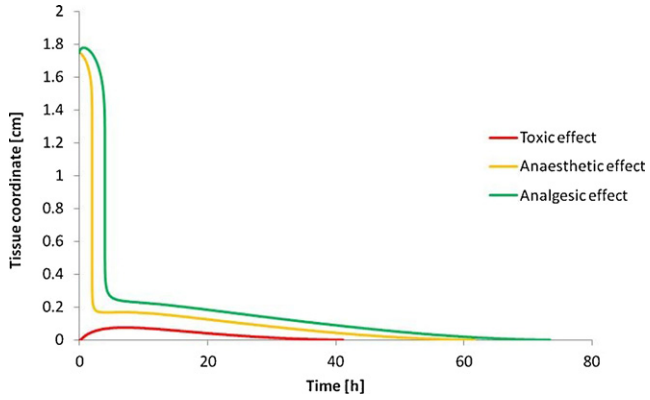

Fig. 7. Phase diagram obtained for a USP 3-0 suture thread in an anesthetized tissue.

2006), and because of the high amount of injected anesthetic, these hypothesis are reasonable as a first approximation for qualitative evaluations. For what concerns the suture thread, input data are coherent with ones presented in Table 2; for the sake of completeness, simulated device is a suture thread made of poly-ε-caprolactone, with an average molecular weight of 80,000 g/mol, a diameter of 0.3 mm (USP 3-0) and a lidocaine load equal to 1% in weight terms. Focusing now on simulation results concerning mass release of drug in time, from plots presented in Fig. 6 it can be immediately seen that a slower release is achieved because of the different driving force to which the thread is subjected.

Focusing on the phase diagram, it can be noticed that the effect of the initial injection rapidly fades and ends after about 5 h, when the device effect begins. Drug release from the thread is then able to extend the anesthetic effects in time, assuring at least an analgesic effect near thread application zone for about 75 h. In this way, indeed, it is possible to guarantee a continuous drug effect from the thread application to the following days, in order to offer a better recovering for the patient. Moreover, the portion of tissue interested by toxic concentrations is extremely limited (see Fig. 7).

4. Conclusions

This work was focused on developing a model capable to describe both the degradation in a tissue of a resorbable suture thread in which an active principle is loaded, and the behavior of the released drug in the tissue. The model has a theoretical nature: it means it is a mathematical representation of all involved phenomena. Thus, parameters have a physical meaning and the model can be used to predict variables trends in other experimental conditions, without losing in validity but with a relevant saving of time and costs. Polymer degradation in water model was taken from literature and used as the starting point to implement the prediction of drug release into a tissue. First of all, influences of thread size and molecular weight on drug release were examined. The effect of thread size is relevant: as diameter increases, release ratio decreases, and thus a slower release is provided; instead, molecular weight effect is negligible as far as delivery characteristic time is always much smaller then degradation one. Simulations data allowed to determine temporal and spatial profile of drug released in tissue and to define phase diagrams, which show drug effect (toxic, anaesthetic, analgesic) in time and space. Furthermore, according to our best knowledge, phase diagrams were here introduced for the first time and proved to be a powerful tool: they offer an easy and immediate view of the effect provided by a certain suture thread, as regard duration in time and distance covered. Influence of drug parameters on active principle effect and drug release was then analyzed. When drug diffusion coefficient in tissue increases, drug effect covers a greater distance but has a lower duration; a similar effect can be achieved by increasing drug half-life time. Moreover, increasing drug diffusion coefficient in tissue and drug half-life time implies a faster release. Influence of these parameters was analyzed quantitatively with a sensitivity analysis. Thanks to the model and its simulations, it is now possible to study the behavior of biodegradable suture threads loaded with different drugs. Models provides predictive data that, without an expensive and time consuming experimental activity, can be easily used as starting point for the final optimization of these kind of devices, speeding up the entire development process but with no loss of safety. The model is, indeed, of general validity, being based on fundamental conservation laws, and thus it can immediately be applied to different biomedical polymers and various drugs.

Appendix A. Supplementary data

Supplementary data associated with this article can be found, in the online version, at doi:10.1016/j.ijpharm.2012.03.024.

References

Alexis, F., 2005. Factors affecting the degradation and drug-release mechanism of poly(lactic acid) and poly[(lactic acid)-co-(glycolic acid)]. Polym. Int. 54, 36–46.
Alexis, F., Kumar Rath, S., Venkatraman, S., 2005. Controlled release from bioerodible polymers: effect of drug type and polymer composition. J. Control. Release 102, 333–344.
Anissimov, Y.G., Roberts, M.S., 2011. Modelling dermal drug distribution after topical application in human. Pharm. Res. 28, 2119–2129.
Arosio, P., Busini, V., Perale, G., Moscatelli, D., Masi, M., 2008. A new model of resorbable device degradation and drug release—part I: zero order model. Polym. Int. 57, 912–920.
Batheja, P., Sheihet, L., Kohn, J., Singer, A.J., Michniak-Kohn, B., 2011. Topical drug delivery by a polymeric nanosphere gel: formulation optimization and in vitro and in vivo skin distribution studies. J. Control. Release 149, 159–167.
Bird, R.B., Stewart, W.E., Lightfoot, E.N., 2002. Transport Phenomena, 2nd ed. Wiley International ed. J Wiley, New York.
Birkett, D.J., 2002. Pharmacokinetics Made Easy. Mc Graw Hill, Australia.
Butts, C.A., Xi, J., Brannigan, G., Saad, A.A., Venkatachalan, S.P., Pearce, R.A., Klein, M.L., Eckenhoff, R.G., Dmochowski, I.J., 2009. Identification of a fluorescent general anesthetic, 1-aminoanthracene. Proc. Natl. Acad. Sci. U.S.A. 106, 6501–6506.
Colombo, P., Bettini, R., Santi, P., DeAscentiis, A., Peppas, N.A., 1996. Analysis of the swelling and release mechanisms from drug delivery systems with emphasis on drug solubility and water transport. J. Control. Release 39, 231–237.
Crank, J., Park, G.S., 1968. Diffusion in Polymers. Academic Press, London, New York.
Crow, B.B., Borneman, A.F., Hawkins, D.L., Smith, G.M., Nelson, K.D., 2005. Evaluation of in vitro drug release, pH change, and molecular weight degradation of poly(L-lactic acid) and poly(D,L-lactide-co-glycolide) fibers. Tissue Eng. 11, 1077–1084.
Dee, K.C., Puleo, D.A., Bizios, R., 2002. An Introduction to Tissue-Biomaterial Interactions. Wiley-Liss, Hoboken, N.J.
Dillow, A.K., Lowman, A.M., 2002. Biomimetic Materials and Design: Biointerfacial Strategies, Tissue Engineering, and Targeted Drug Delivery. Marcel Dekker, New York.
DuBose, J.W., Cutshall, C., Metters, A.T., 2005. Controlled release of tethered molecules via engineered hydrogel degradation: model development and validation. J. Biomed. Mater. Res. Part A 74A, 104–116.

Faisant, N., Siepmann, J., Benoit, J.P., 2002. PLGA-based microparticles: elucidation of mechanisms and a new, simple mathematical model quantifying drug release. Eur. J. Pharm. Sci. 15, 355–366.
Frank, A., Rath, S.K., Venkatraman, S.S., 2005. Controlled release from bioerodible polymers: effect of drug type and polymer composition. J. Control. Release 102, 333–344.
Fredenberg, S., Wahlgren, M., Reslow, M., Axelsson, A., 2011. The mechanisms of drug release in poly(lactic-co-glycolic acid)-based drug delivery systems—a review. Int. J. Pharm. 415, 34–52.
Freiberg, S., Zhu, X., 2004. Polymer microspheres for controlled drug release. Int. J. Pharm. 282, 1–18.
Garcia, X., Escribano, E., Domenech, J., Queralt, J., Freixes, J., 2011. In vitro characterization and in vivo analgesic and anti-allodynic activity of PLGA-bupivacaine nanoparticles. J. Nanopart. Res. 13, 2213–2223.
Goldstein, R.P., Amundson, N.R., 1965. An analysis of chemical reactor stability and control. Chem. Eng. Sci. 20, 195–236.
Goodman, L.S., Gilman, A., Brunton, L.L., Lazo, J.S., Parker, K.L., 2006. Goodman & Gilman's the Pharmacological Basis of Therapeutics, 11th ed. McGraw-Hill, New York.
Grassi, G., Hasa, D., Voinovich, D., Perissutti, B., Dapas, B., Farra, R., Franceschinis, E., Grassi, M., 2010. Simultaneous release and ADME processes of poorly water-soluble drugs: mathematical modeling. Mol. Pharm. 7, 1488–1497.
Grassi, M., Grassi, R., Lapasin, R., Colombo, I., 2008. Understanding Drug Release and Absorption Mechanisms. CRC Press, Boca Raton, USA.
Grayson, A.C.R., Cima, M.J., Langer, R., 2005. Size and temperature effects on poly(lactic-co-glycolic acid) degradation and microreservoir device performance. Biomaterials 26, 2137–2145.
Grizzi, I., Garreau, H., Li, S., Vert, M., 1995. Hydrolytic degradation of devices based on poly(DL-lactic acid) size-dependence. Biomaterials 16, 305–311.
Haik-Creguer, K.L., Dunbar, G.L., Sabel, B.A., Schroeder, U., 1998. Small drug sample fabrication of controlled release polymers using the microextrusion method. J. Neurosci. Methods 80, 37–40.
Helbling, I.M., Luna, J.A., Cabrera, M.I., 2011. Mathematical modeling of drug delivery from torus-shaped single-layer devices. J. Control. Release 149, 258–263.
Holy, C.E., Dang, S.M., Davies, J.E., Shoichet, M.S., 1999. In vitro degradation of a novel poly(lactide-co-glycolide) 75/25 foam. Biomaterials 20, 1177–1185.
Kamaya, H., Hayes, J.J., Ueda, I., 1983. Dissociation-constants of local-anesthetics and their temperature-dependence. Anesth. Analg. 62, 1025–1030.
Kaunisto, E., Marucci, M., Borgquist, P., Axelsson, A., 2011. Mechanistic modelling of drug release from polymer-coated and swelling and dissolving polymer matrix systems. Int. J. Pharm. 418, 54–77.
Kim, K.S., Simon, L., 2011. Modeling and design of transdermal drug delivery patches containing an external heating device. Comput. Chem. Eng. 35, 1152–1163.
Kretsos, K., Kasting, G.B., Nitsche, J.M., 2004. Distribution diffusion-clearance model for transient drug distribution within the skin. J. Pharm. Sci. 93, 2820–2835.
Krewson, C.E., Saltzman, W.M., 1996. Transport and elimination of recombinant human NGF during long-term delivery to the brain. Brain Res. 727, 169–181.
Kuttler, A., Dimke, T., Kern, S., Helmlinger, G., Stanski, D., Finelli, L.A., 2010. Understanding pharmacokinetics using realistic computational models of fluid dynamics: biosimulation of drug distribution within the CSF space for intrathecal drugs. J Pharmacokinet. Pharmacodyn. 37, 629–644.
Lao, L.L., Peppas, N.A., Boey, F.Y.C., Venkatraman, S.S., 2011. Modeling of drug release from bulk-degrading polymers. Int. J. Pharm. 418, 28–41.
Lee, H., Hoang, B., Fonge, H., Reilly, R.M., Allen, C., 2010. In vivo distribution of polymeric nanoparticles at the whole-body, tumor, and cellular levels. Pharm. Res. 27, 2343–2355.
LeVeque, R.J., 2007. Finite Difference Methods for Ordinary and Partial Differential Equations. Society for Industrial and Applied Mathematics, Philadelphia.
Li, S.M., Garreau, H., Vert, M., 1990. Structure property relationships in the case of the degradation of massive aliphatic poly-(alpha-hydroxy acids) in aqueous-media. 1. Poly(DL-lactic acid). J. Mater. Sci. Mater. Med. 1, 123–130.
Li, Z.H., Alex, D., Siu, S.O., Chu, I.K., Renn, J., Winkler, C., Lou, S., Tsui, S.K.W., Zhao, H.Y., Yan, W.R., Mahady, G.B., Li, G.H., Kwan, Y.W., Wang, Y.T., Lee, S.M.Y., 2011. Combined in vivo imaging and omics approaches reveal metabolism of icaritin and its glycosides in zebrafish larvae. Mol. Biosyst. 7, 2128–2138.
Loney, N.W., Susarla, R., 2009. Mathematical modeling of drug release from spherical drug particles: analysis of the effect of absorption rate on drug release rate. Chem. Prod. Process Model. 4.
Meriani, F., Coceani, N., Sirotti, C., Voinovich, D., Grassi, M., 2004. In vitro nimesulide absorption from different formulations. J. Pharm. Sci. 93, 540–552.
Miller-Chou, B.A., Koenig, J.L., 2003. A review of polymer dissolution. Prog. Polym. Sci. 28, 1223–1270.
Mitragotri, S., 2000. In situ determination of partition and diffusion coefficients in the lipid bilayers of stratum corneum. Pharm. Res. 17, 1026–1029.
Monkare, J., Hakala, R.A., Vlasova, M.A., Huotari, A., Kilpelainen, M., Kiviniemi, A., Meretoja, V., Herzig, K.H., Korhonen, H., Seppala, J.V., Jarvinen, K., 2010. Biocompatible photocrosslinked poly(ester anhydride) based on functionalized poly (epsilon-caprolactone) prepolymer shows surface erosion controlled drug release in vitro and in vivo. J. Control. Release 146, 349–355.
Musial, W., Kokol, V., Voncina, B., 2010. Lidocaine hydrochloride preparations with ionic and non-ionic polymers assessed at standard and increased skin surface temperatures. Chem. Papers 64, 84–90.
Noorsal, K., Mantle, M.D., Gladden, L.F., Cameron, R.E., 2005. Degradation and drug-release studies of a poly(glycolide-co-trimethylene carbonate) copolymer (Maxon). J. Appl. Polym. Sci. 95, 475–486.
Numata, K., Finne-Wistrand, A., Albertsson, A.C., Doi, Y., Abe, H., 2008. Enzymatic degradation of monolayer for poly(lactide) revealed by real-time atomic force microscopy: effects of stereochemical structure, molecular weight, and molecular branches on hydrolysis rates. Biomacromolecules 9, 2180–2185.
Pavlisa, G., Rados, M., Pavlisa, G., Pavic, L., Potocki, K., Mayer, D., 2009. The differences of water diffusion between brain tissue infiltrated by tumor and peritumoral vasogenic edema. Clin. Imaging 33, 96–101.
Perale, G., Arosio, P., Moscatelli, D., Barri, V., Muller, M., Maccagnan, S., Masi, M., 2009. A new model of resorbable device degradation and drug release: transient 1-dimension diffusional model. J. Control. Release 136, 196–205.
Perale, G., Casalini, T., Barri, V., Muller, M., Maccagnan, S., Masi, M., 2010. Lidocaine release from polycaprolactone threads. J. Appl. Polym. Sci. 117, 3610–3614.
Perale, G., Pertici, G., Giordano, C., Daniele, F., Masi, M., Maccagnan, S., 2008. Non-degradative microextrusion of resorbable polyesters for pharmaceutical and biomedical applications: the cases of poly-lactic-acid and poly-caprolactone. J. Appl. Polym. Sci. 108, 1591–1595.
Perale, G., Rossi, F., Santoro, M., Peviani, M., Papa, S., Llupi, D., Torriani, P., Micotti, E., Previdi, S., Cervo, L., Sundstrom, E., Boccaccini, A.R., Masi, M., Forloni, G., Veglianese, P. Multiple drug delivery hydrogel system for spinal cord injury repair strategies. J. Control. Release, in press.
Pitt, G.C., 1992. Biodegradable Polymers and Plastic. Royal Society of Chemistry, London, UK.
Posnansky, O.P., Shah, N.J., 2008. On the problem of diffusivity in heterogeneous biological materials with random structure. J. Biol. Phys. 34, 551–567.
Powell, M.F., 1987. Stability of lidocaine in aqueous-solution—effect of temperature, pH, buffer, and metal-ions on amide hydrolysis. Pharm. Res. 4, 42–45.
Ramkrishna, D., 2000. Population Balances. Academic Press, San Diego, USA.
Remington, J.P., 1995. Remington, the Science and Practice of Pharmacy. Mack Pub. Co., Easton, PA.
Rothstein, S.N., Federspiel, W.J., Little, S.R., 2009. A unified mathematical model for the prediction of controlled release from surface and bulk eroding polymer matrices. Biomaterials 30, 1657–1664.
Sackett, C.K., Narasimhan, B., 2011. Mathematical modeling of polymer erosion: consequences for drug delivery. Int. J. Pharm. 418, 104–114.
Saltzman, W.M., Mak, M.W., Mahoney, M.J., Duenas, E.T., Cleland, J.L., 1999. Intracranial delivery of recombinant nerve growth factor: release kinetics and protein distribution for three delivery systems. Pharm. Res. 16, 232–240.
Semete, B., Booysen, L., Lemmer, Y., Kalombo, L., Katata, L., Verschoor, J., Swai, H.S., 2010. In vivo evaluation of the biodistribution and safety of PLGA nanoparticles as drug delivery systems. Nanomed-Nanotechnol. 6, 662–671.
Shin, B.S., Bulitta, J.B., Balthasar, J.P., Kim, M., Choi, Y., Yoo, S.D., 2011. Prediction of human pharmacokinetics and tissue distribution of apicidin, a potent histone deacetylase inhibitor, by physiologically based pharmacokinetic modeling. Cancer. Chemother. Pharmacol. 68, 465–475.
Siegel, S.J., Kahn, J.B., Metzger, K., Winey, K.I., Werner, K., Dan, N., 2006. Effect of drug type on the degradation rate of PLGA matrices. Eur. J. Pharm. Biopharm. 64, 287–293.
Siepmann, J., Gopferich, A., 2001. Mathematical modeling of bioerodible, polymeric drug delivery systems. Adv. Drug Deliv. Rev. 48, 229–247.
Siepmann, J., Siepmann, F., Florence, A.T., 2006. Local controlled drug delivery to the brain: mathematical modeling of the underlying mass transport mechanisms. Int. J. Pharm. 314, 101–119.
Sjoberg, H., Karami, K., Beronius, P., Sundelof, L.O., 1996. Ionization conditions for iontophoretic drug delivery. A revised pK(a) of lidocaine hydrochloride in aqueous solution at 25 °C established by precision conductometry. Int. J. Pharm. 141, 63–70.
Soares, J.S., Zunino, P., 2010. A mixture model for water uptake, degradation, erosion and drug release from polydisperse polymeric networks. Biomaterials 31, 3032–3042.
Sokolsky-Papkov, M., Agashi, K., Olaye, A., Shakesheff, K., Domb, A.J., 2007. Polymer carriers for drug delivery in tissue engineering. Adv. Drug Deliv. Rev. 59, 187–206.
Song, C., Gu, H., Long, D., Mei, L., Sun, H., 2007. Controlled release of recombinant human nerve growth factor (rhNGF) from poly[(lactic acid)-co-(glycolic acid)] microspheres for the treatment of neurodegenerative disorders. Polym. Int. 56, 1272–1280.
Streubel, A., Siepmann, J., Peppas, N.A., Bodmeier, R., 2000. Bimodal drug release achieved with multi-layer matrix tablets: transport mechanisms and device design. J. Control. Release 69, 455–468.
Tessmar, J.K., Gopferich, A.M., 2007. Matrices and scaffolds for protein delivery in tissue engineering. Adv. Drug Deliv. Rev. 59, 274–291.
Thombre, A.G., Himmelstein, K.J., 1985. A simultaneous transport-reaction model for controlled drug delivery from catalyzed bioerodible polymer matrices. AICHE J. 5, 759–766.
Tojo, K., Aoyagi, H., Kurita, T., 1998. Surface dissolution-bulk erosion model of drug release from biodegradable polymer rods. J. Chem. Eng. Jpn. 31, 648–651.
Tsuji, H., Tezuka, Y., 2004. Alkaline and enzymatic degradation of L-lactide copolymers, 1—amorphous-made films of L-lactide copolymers with D-lactide, glycolide, and epsilon-caprolactone. Macromol. Biosci. 5, 135–148.
Tsuji, H., Tezuka, Y., Yamada, K., 2005. Alkaline and enzymatic degradation of L-lactide copolymers. II. Crystallized films of poly(L-lactide-co-D-lactide) and poly(L-lactide) with similar crystallinities. J. Polym. Sci. Part B: Polym. Phys. 43, 1064–1075.
von Burkersroda, F., Schedl, L., Gopferich, A., 2002. Why degradable polymers undergo surface erosion or bulk erosion. Biomaterials 23, 4221–4231.

Vrentas, J.S., Vrentas, C.M., 1998. Dissolution of rubbery and glassy polymers. J. Polym. Sci. Part B: Polym. Phys. 36, 2607–2614.
Wang, Y.L., Wang, L.Y., Han, Y.F., Henderson, S.C., Majeska, R.J., Weinbaum, S., Schaffler, M.B., 2005. In situ measurement of solute transport in the bone lacunar–canalicular system. Proc. Natl. Acad. Sci. U.S.A. 102, 11911–11916.
Westedt, U., Wittmar, M., Hellwig, M., Hanefeld, P., Greiner, A., Schaper, A.K., Kissel, T., 2006. Paclitaxel releasing films consisting of poly(vinyl alcohol)-graft-poly(lactide-co-glycolide) and their potential as biodegradable stent coatings. J. Control. Release 111, 235–246.
Willerth, S.M., Sakiyama-Elbert, S.E., 2007. Approaches to neural tissue engineering using scaffolds for drug delivery. Adv. Drug Deliv. Rev. 59, 325–338.
Zurita, R., Puiggali, J., Rodriguez-Galan, A., 2006a. Loading and release of ibuprofen in multi- and monofilament surgical sutures. Macromol. Biosci. 6, 767–775.
Zurita, R., Puiggali, J., Rodriguez-Galan, A., 2006b. Triclosan release from coated polyglycolide threads. Macromol. Biosci. 6, 58–69.